Elsevier Editorial System(tm) for Journal of Non-Crystalline Solids or its open access mirror
Manuscript Draft

Manuscript Number: NOC-D-20-00270

Title: Compositional Dependence of Red Photoluminescence of Eu3+ Ions in Lead and Bismuth Containing Borate Glasses

Article Type: Full Length Article

Keywords: Borate Glasses; Heavy Metal Oxides; Europium; Photoluminescence; Judd-Ofelt theory; Quantum efficiency.

Corresponding Author: Dr. Kokila M K, Ph.D

Corresponding Author's Institution: Bangalore University

First Author: Kokila M K, Ph.D

Order of Authors: Kokila M K, Ph.D; P Ramesh, M.Phill; Vinod Hegde, M.Sc.; A.G Pramod, Ph.D.; B Eraiah, Ph.D.; D.A Agarkov, Ph.D.; G.M Eliseeva, M.Sc.; M.K Pandey, Ph.D.; K Annapurna, Ph.D.; G Jagannath, Ph.D.

Abstract: Herein, the borate glasses containing high concentration of heavy metal oxides activated with different concertation of Eu2O3 were prepared via rapid melt quench method. The Eu3+ concentration effect on photoluminescence (PL) properties of prepared glasses were investigated and discussed in details to understand their utility in solid-state lighting and other photonic applications. The Judd-Ofelt parameters and the radiative properties suggest the heavy metal borate glass hosts activated with 1 mol % of Eu3+ were potential materials for red light emitting devices under blue light excitations. The Lifetime and quantum efficiency values of the PbO framed glasses were greater compared to Bi2O3 framed borate glasses which suggest the borate glass host containing high PbO content are more precisely suitable than Bi2O3 containing borate glass for solid state lighting applications under blue light excitation.

Suggested Reviewers: Dr. José M.F. Ferreira Ph.D.
Professor, Department of Materials and Ceramics Engineering, University of Aveiro
jmf@ua.pt
Prof. José M.F. Ferreira is the expert in glass and glass-ceramic materials

Dr. Amarnath R Allu Ph.D.
Scientist, Glass Division, CSIR-Central Glass and Ceramic Research Institute Kolkata
aareddy@cgcri.res.in
Dr. Amarnath R Allu is the expert in analysing the properties of glasses

Dr. Swart H C Ph.D.
Professor, Department of Physics, University of the Free State
SwartHC@ufs.ac.za

Prof. H C Swart is the expert in analysing the luminescence properties of materials.

Dear Sir / Madam,

We are submitting our manuscript entitled "**Compositional Dependence of Red Photoluminescence of Eu^{3+} Ions in Lead and Bismuth Containing Borate Glasses**" by P. Ramesh, Vinod Hegde, A.G. Pramod, B. Eraiah, D.A. Agarkov, G.M. Eliseeva, Sudipta Som, M. K. Pandey, K. Annapurna, G. Jagannath, and M.K. Kokila, which we think is suitable for publication in the **Journal of Non-Crystalline Solids**. I would like to declare that I have the consent of my co-authors to submit this original article to your journal and affirm that it has not been submitted for publication elsewhere.

The borate glasses containing high concentration of heavy metal oxides activated with different concertation of Eu_2O_3 were prepared via rapid melt quench method. The Eu^{3+} concentration effect on photoluminescence (PL) properties of prepared glasses were investigated and discussed in detail to understand their utility in solid-state lighting and other photonic applications. The PL intensity was increased with increase in Eu^{3+} content in PbO framed borate glasses while in bismuth containing borate glasses the PL intensity was decreased at higher concentration due to concentration quenching. Further, there are large number of reports in open literature on PL and spectroscopic properties of Eu^{3+} doped glasses excited at Ultra-Violet (UV) light. However, there are very few reports are available under blue light excitation. Furthermore, it is important to investigate the PL properties of Eu^{3+} doped heavy metal oxide containing glasses at both the excitations (UV and blue light) to demonstrate the glasses for device application more potentially. Therefore, in present study the PL properties of borate glasses containing high concentration of PbO and Bi_2O_3 activated with different concentration of Eu^{3+} ions are studied at dual excitations and discussed in detail for red solid-state lighting applications.

We strongly believe that this manuscript is appropriate for publication in the **Journal of Non-Crystalline Solids**, since this journal covers all aspects of production material or the properties or applications of materials related different applications including PL and spectroscopic properties for photonic applications. To the best of our knowledge, no similar studies have been reported so far in the open literature.

If you require any further information regarding this manuscript, please do not hesitate to contact us.

We look forward to hear a favorable reply from you.

Please note that your future correspondence should be addressed to:

Prof. M K Kokila
Department of Physics,
Bangalore University, 560056,
Bengaluru, Karnataka, India
Email: mkkokila659@gmail.com
Phone: +91-8022961485

Journal of
Non-Crystalline Solids

Confirmation of Authorship

As corresponding author, I **Dr. M K Kokila**, hereby confirm on behalf of all authors that:

1. This manuscript has not been published, was not, and is not being submitted to any other journal. If presented at a conference, the conference is identified. If published in conference proceedings, substantial justification for re-publication must be presented.

2. All necessary permissions for publication were secured prior to submission of the manuscript.

3. All authors listed have made a significant contribution to the research reported and have read and approved the submitted manuscript, and furthermore, all those who made substantive contributions to this work have been included in the author list.

*Abstract

Compositional Dependence of Red Photoluminescence of Eu^{3+} Ions in Lead and Bismuth Containing Borate Glasses

Abstract: Herein, the borate glasses containing high concentration of heavy metal oxides activated with different concertation of Eu_2O_3 were prepared via rapid melt quench method. The Eu^{3+} concentration effect on photoluminescence (PL) properties of prepared glasses were investigated and discussed in details to understand their utility in solid-state lighting and other photonic applications. The Judd–Ofelt parameters and the radiative properties suggest the heavy metal borate glass hosts activated with 1 mol % of Eu^{3+} were potential materials for red light emitting devices under blue light excitations. The Lifetime and quantum efficiency values of the PbO framed glasses were greater compared to Bi_2O_3 framed borate glasses which suggest the borate glass host containing high PbO content are more precisely suitable than Bi_2O_3 containing borate glass for solid state lighting applications under blue light excitation.

Keywords: Borate Glasses; Heavy Metal Oxides; Europium; Photoluminescence; Judd–Ofelt theory; Quantum efficiency.

Highlights

- Photoluminescence properties of Eu^{3+} ions in borate glasses containing high concentration of PbO and Bi_2O_3 were investigated under UV light and blue light excitations.

- The PbO containing glasses activated with 1 mol % of Eu_2O_3 demonstrated improved Judd-Ofelt parameters along with high quantum efficiency and life time than Bi_2O_3 containing glasses.

- The Judd-Ofelt analysis suggest the PbO containing glasses are more beneficial for solid state lighting application than Bi_2O_3 containing glasses under blue light excitation.

Compositional Dependence of Red Photoluminescence of Eu^{3+} Ions in Lead and Bismuth Containing Borate Glasses

P. Ramesh[1,2], Vinod Hegde[3], A.G. Pramod[1], B. Eraiah[1], D.A. Agarkov[4,5,*], G.M. Eliseeva[4], M.K. Pandey[6,*], K. Annapurna[7], G. Jagannath[8], and M.K. Kokila[1,*]

[1] Department of Physics, Bangalore University, Bangalore 560056, Karnataka, India.

[2] Govt. College for Women, Kolar 563101, Karnataka, India.

[3] Department of Physics, Acharya Institute of Graduate Studies, Bangalore 560107, India

[4] Institute of Solid State Physics RAS, 142432 Chernogolovka, Moscow District, Russia

[5] Moscow Institute of Physics and Technology, 141701 Dolgoprudny, Moscow District, Russia

[6] Department of Physics, Center for Theoretical Physics, National Taiwan University, Taipei 10617, Taiwan.

[7] Glass Division, CSIR-Central Glass and Ceramic Research Institute, Kolkata 700032, India.

[8] Department of Physics, K S Institute of Technology, Bangalore 560109, Karnataka, India.

Corresponding Authors

*E-mail: mkpandey@gmail.com (MKP)

*E-mail: agarkov@issp.ac.ru (DAA)

*E-mail: drmkkokila@gmail.com (MKK)

Abstract: Herein, the borate glasses containing high concentration of heavy metal oxides activated with different concertation of Eu_2O_3 were prepared via rapid melt quench method. The Eu^{3+} concentration effect on photoluminescence (PL) properties of prepared glasses were investigated and discussed in details to understand their utility in solid-state lighting and other photonic applications. The Judd–Ofelt parameters and the radiative properties suggest

the heavy metal borate glass hosts activated with 1 mol % of Eu^{3+} were potential materials for red light emitting devices under blue light excitations. The Lifetime and quantum efficiency values of the PbO framed glasses were greater compared to Bi_2O_3 framed borate glasses which suggest the borate glass host containing high PbO content are more precisely suitable than Bi_2O_3 containing borate glass for solid state lighting applications under blue light excitation.

Keywords: Borate Glasses; Heavy Metal Oxides; Europium; Photoluminescence; Judd–Ofelt theory; Quantum efficiency.

1. Introduction

Search for an efficient optical material for the solid–state lighting and laser applications has become growing interest from past decades to address the technological challenges in opto-electronics devices, display devices, optical amplifiers and many more. Recently, solid-state optical materials are used for spectral conversion such as wavelength up and down conversion processes etc. [1–4]. Interestingly, optical materials comprising of rare earth (RE)s were applied as light gain medium for near infrared solid state laser, optical amplifier, optical thermometry and many photonic devices [5–9]. In particular, the high power visible light emitting solid–state devices are crucial for pool lights, headlights and architecture lighting applications[10,11].

Among the different systems bearing relevant interest in photonics [12–15], the use of glasses as dielectric hosts for RE ions has some advantages over other systems, such as high transparency in selective electromagnetic fields, mechanical and chemical strength, possibility of production of devices on several shapes and the absence of metal–ligand interactions (causes quenching processes due to the high energy stretching vibrations) [16].

Especially, for the artificial lighting devices, moisture and heat resistant oxide glasses doped with RE ions are the excellent choice [17–19]. In view of this, the borate based glasses are of significant interest owing to their good optical transparency, chemical, thermal and mechanical, stability [20] along with low melting and processing temperatures. It is well known that, the local environment and its variation, as well as the concentration and distribution of the RE ion in the glass matrix influence the luminescence properties such as emission intensity, quantum efficiency, emission cross section, spectral line width and life time. Therefore, these properties play a vital role while selecting the RE doped glasses for photonic applications [21]. To this end also, the borate-based glasses are good choice as a host for the REs since they constituted with a wide range of compositions without the addition of any network modifiers. Nonetheless, the distinct structural units of borate glasses such as BO_3 triangle and BO_4 tetrahedra helps to improve the local crystal field around the RE^{3+} ions [22]. However, the borate glasses contain high energy phonons (1300–1500 cm^{-1}) [20], which negatively influence the quantum yield of photoluminescence (PL) of RE ions and hence limits the practical utility of borate glasses in photonic applications. To achieve the high quantum yield of PL of RE ions, it is desirable that the RE should locate in a low phonon energy environment, so that the probability of nonradiative transitions can be reduced, subsequently resulting to high PL efficiency [23]. It has been well reported that, the incorporation of heavy metal oxides (HMOs) such as Bi_2O_3, PbO, Sb_2O_3, CdO etc. reduces the phonon energy of the parent glass and thereby enhances the optical as well as spectroscopic properties RE activated glasses. In addition, the HMOs improves the transparency of the parent glass in the infrared regions [24–27].

Among all RE ions, trivalent europium ions (Eu^{3+}) are of great importance as they exhibit efficient and intense red–orange emission originating from both electric dipole (ED, $^5D_0 \rightarrow {}^7F_1$) and magnetic dipole (MD, $^5D_0 \rightarrow {}^7F_1$) transitions with often high quantum

efficiency. Also the Eu^{3+} is used in persistent spectral hole burning, luminescent devices and in high–density optical storage components [28,29]. Nonetheless, the band energy of the *f–f* transitions is generally not related to ligand field strength and, therefore, the host material, the ED allowed transition of Eu^{3+}: $^5D_0 \rightarrow {}^7F_2$ strongly related to local symmetry. As a result, this $^5D_0 \rightarrow {}^7F_2$ transition can be utilized to probe the local structure in the host material. For this, the relative PL intensity ratio of I_{02}/ I_{01} transitions (often denoted as the asymmetry ratio, R) is widely employed to estimate the degree of non–centro symmetry of the Eu^{3+} site in a host material [30]. Normally, the absorption cross section of Eu^{3+} is very small in the ultra violet (UV) range due to parity–forbidden nature of Eu^{3+} absorption that result in low efficiency emission under the UV excitation and therefore, limits their versatility in many applications. Increasing the Eu^{3+} doping concentration in the host material is one way to overcome this problem, but which may causes the concentration quenching of PL emission [29]. However, the incorporation of glass modifiers and/or formers with higher concentration is an alternative way to overcome this problem. Nevertheless, Hirdesh et. al. [31] have observed the excitation dependence PL properties of Eu^{3+} activated in heavy metal oxide glasses. Yu et. al. [32] have further confirmed that the PL intensity of Eu^{3+} is maximum at the excitation of blue light than ultra–violet (UV) light in heavy metal oxide glasses. To this end, there are few reports are available in open literature on PL and spectroscopic properties of Eu^{3+} doped glasses excited at blue light. Furthermore, it is important to investigate the PL properties of Eu^{3+} doped heavy metal oxide containing glasses at both the excitations (UV and blue light) to demonstrate the glasses for device application more potentially. Therefore, in present study the PL properties of borate glasses containing high concentration of PbO and Bi_2O_3 activated with different concentration of Eu^{3+} ions are studied at dual excitations and discussed in detail for red solid-state lighting applications.

2. Experimental and characterization details

Eu_2O_3 varied series of glass samples with chemical formula $10La_2O_3$–50HMO–(40–x)B_2O_3–xEu_2O_3 (with x = 0, 0.5, 1 and 2 mol % and HMO = PbO, Bi_2O_3) were fabricated through the process of melt-quenching in porcelain crucibles. The labels for the prepared samples are LPb50BEu*x* and LBi50BEu*x* for the lead and bismuth containing samples respectively, here *x* indicates the concentration of Eu_2O_3 in the glass system. The Eu_2O_3 free samples are labelled as LPb50B and LBi50B for lead and bismuth containing glasses respectively. The starting reagents of high grade oxides such as B_2O_3, PbO, La_2O_3 and Eu_2O_3 were procured from SD Fine Chemicals Ltd. for glass preparation and same were used without additional purification. The weighted 15 gms of glass composition was grinded thoroughly for homogenous. The well mixed glass mixture transferred to porcelain crucible and kept for melting using muffle furnace. The lead containing glass mixture was melted at 1050 °C and bismuth containing glass mixture was melted at 1030 °C. After 20 min of melting, molten mass was quenched on pre heated (200 °C) brass molds. The obtained glass samples were heat treated for 4 hours at 450 °C to distress glass structure occurred while quenching. Later, the glass samples were finely polished using various grade emery sheets. The samples were optically homogeneous to naked eyes and free from strains occurred due to the high melt temperatures, large melting time, and low cooling rates.

Density and refractive index measurement of the prepared glasses carried out by utilising Archimedes' principle (comprising of analytical balance and toluene as immersion liquid) and Abbe's refractometer (measured at 589.3 nm) respectively. Optical absorption spectra of all the prepared glass samples were recorded using PerkinElmer Lambda–35 UV–Vis spectrometer. The identification of structural groups formed in the glass network was carried–through Fourier transform infrared (FTIR) transmission and Raman scattering measurement using home-made setup described elsewhere [33–35]. PL excitation and

emission spectra were collected using an YvonFluorolog 3 spectrofluorimeter having a 450 W Xenon flash lamp as the exiting source

3. Result and Discussion

3.1. Physical properties

The prepared glass samples were checked for glassy nature using X–Ray Diffractometer (XRD). The XRD profiles of the Eu free samples and samples containing 1 mol % of Eu^{3+} are shown figure 1. The samples were demonstrated a broad hump with absence of sharp crystalline peaks suggest the investigated glass samples are amorphous in nature. The glass becomes luminescent material when it contains optically active ions such as Eu^{3+} in its network. The oxide form of Eu_2O_3 has been taken to dope the Eu^{3+} ion in the PbO and Bi_2O_3 borate glass network. The doping process carried out by replacing the B_2O_3 by 0.5, 1 and 2 mol % Eu_2O_3. The Eu^{3+} ion is differed by its ionic radii, molar mass and electro–negativity compared to B^{3+} and thereby affect the bonding of the glass network. Thus, physical properties of the glass such as density, refractive index are measured and other properties were calculated using the equations mentioned in the references [36,37].

The undoped glasses are heavily dense compared to respective RE doped glasses. From the Table 1 it is evident that density values of LPb50BEu*x* and LBi50BEu*x* glasses are decreased as Eu^{3+} doping level increased from 0.5 to 2 mol %. The refractive index and molar volume of the glasses are increased as Eu^{3+} ions entered the network and it is highest for 2 mol % Eu^{3+} doped glasses. The other properties of the glasses such as dielectric constant, molar refractivity and electronic polarizability of the glasses increased with doping concentration of Eu^{3+} ion. Meanwhile, inter–ionic distance between the Eu^{3+} ions is decreased in lead as well as in bismuth lanthanum borate glass. These changes are attributed to the structural re–arrangement occurred in the Eu^{3+} doped PbO and Bi_2O_3 containing borate

glasses. The increase in refractive index and polarizability values shows the enhancement in the light interaction with the glassy structure. These changes are due to decrease of bridging oxygen's over non–bridging oxygen's (NBO's). The NBO's in the network provides more scope for light–matter interaction through its less bounded excited electrons [38]. Further, the bismuth containing samples are highly dense compared lead comprising samples which is due to the greater atomic mass of Bi_2O_3 (465.96 amu) compared to PbO (223.2 amu). Also, the molar volume values of the LBi50BEu*x* glasses are greater compared to those of LP50BEu*x*, this is because the Bi–O (ranges from 2.08–2.80 Å) bond lengths are higher compared to Pb–O (in the range of 2.18–2.49 Å) bond lengths [39].

3.2. Structural Properties

3.2.1. Fourier transform infrared (FTIR) spectroscopy

FTIR spectra of LPb50B and LBi50B glasses are shown in Fig. 2 (a). There are three main bands in the figure which are in agreement with those found in references [40–42] but of better resolution that allows assignments of the various bands. It was greatly accepted that the broad band around 1100–1500 cm^{-1} is ascribed to stretching vibration of B–O bonds of trigonal $(BO_3)^{3-}$ groups in metaborate, pyroborate and orthoborates [40], whereas the band around 750–1100 cm^{-1} is attributed to stretching vibration of B–O bonds in tetrahedral $(BO_4)^{-}$ groups [43]. The transmission band at around 690–700 cm^{-1} is due to the bending vibrations of the B–O linkages in the borate network [40]. The weak band or the kink at 621 cm^{-1} observed in lead containing glass was attributed to bending vibration of O–B–O bonds of borate units [44]. Nevertheless, the IR analysis of the Bi_2O_3 containing glasses demonstrated a weak bands in low frequency region extended between 500–600 cm^{-1} which are attributed to bending vibrations of Bi–O–Bi bonds in highly distorted BiO_6 octahedral units [45,46]. By the keen observation of IR spectra, it was evident that, the centres of the 750–1100 cm^{-1} and 1150–1500 cm^{-1} bands in bismuth containing glass were slightly shifted

to lower wave number with reduced width compared to lead containing sample. It has been reported that, the centre of the band around 750–1100 cm^{-1} shifted to lower wave number indicating an increase in NBOs, and a longer bond length of BO_4 structural unit. While, the center of the same band shifted to higher wave number indicating a decrease in NBOs and a shortening in the bond length of BO_4 [46]. Therefore, the shift of 760 –1100 cm^{-1} band to lower wave number is attributed to increase in NBOs and a lengthening in the bond length of BO_4 when Bi_2O_3 incorporated in the place of PbO. Further, the shift of 1150–1500 cm^{-1} band towards the lower wave number in Bi_2O_3 containing sample may be due to the fact that, the new bridging bond of Bi–O–B is formed by the inducement of strongly polarizing Bi^{3+} ions. Since the stretching force constant of Bi –O bonding is substantially lower than that of the Pb–O, hence the stretching frequency of Bi–O–B might trend to be lower [45,47,48].

3.2.2. Raman spectroscopy

The Raman spectra of Eu^{3+} free LPb50B and LBi50B glasses are shown in Fig. 2 (b). The spectra of both hosts evidenced the absence of the boroxol characteristic band at ~ 805 cm^{-1} [41], which represents the glasses under study are not containing any boroxol rings. The broad Raman signal observed at around ~ 1252 cm^{-1} was attributed to the pyroborate structural units ($B_2O_5^{4-}$)[49,50]. This band is slightly shifted to lower wavenumber in Bi_2O_3 containing glass system. This shift suggest an increasing depolymerization and an increasing number of NBOs sites in bismuth containing glass sample [51]. The Raman lines appeared at ~ 935 cm^{-1} and at ~ 900 cm^{-1} (present in lead containing sample only) were attributed to symmetric stretching vibration of the planar orthoborate units (BO_3^{3-}) units [52]. The weak bands appeared at ~ 628 cm^{-1} in lead containing sample was attributed to ring type metaborate groups [41]. The Raman bands observed at ~ 710 (~718 cm^{-1} in bismuth containing host) and ~ 731 cm^{-1} were ascribed to chain type metaborate units [41]. The identified weak peak at ~ 761 cm^{-1} in lead containing host reveals the presence of a BO_4

structural groups units, probably in diborate groups [53]. The Raman band present at ~ 490 cm^{-1} in PbO comprising glass host was ascribed to loose' diborate groups and 'loose' BO_4 group [54]. The band observed at ~ 595 cm^{-1} in LPb50B glasses was ascribed to isolated diborate units [53]. Finally, the weak intense band developed at ~ 240 and ~ 315 cm^{-1} in lead containing sample could be ascribed to the vibrational mode of Pb^{2+} in fourfold coordination [51]. This developed Raman bands at low frequency region is also indicate the gradual growth of a PbO_n pseudo phase within the glass matrix; for high PbO concentration this may take the form of PbO_4 square-pyramidal structures with considerable degree of covalent Pb–O bonding [55]. The Raman band appeared at ~ 790 cm^{-1} in LBi50B glass could be assigned to the vibration of planar six membered borate rings with one BO_4 tetrahedron [41]. The band observed at ~ 432 cm^{-1} in bismuth containing sample assigned to stretching vibrations of Bi−O−Bi linkages of BiO_6 octahedron [56]. The peak developed at ~ 263 cm^{-1} in LBi50B glass could be assigned for vibration of Bi-O bond in [BiO_3] structural unit [57]. No clear assignment of the weak Raman line appeared at ~ 680 cm^{-1} in bismuth containing glass sample. Because, the formation of [$B\Theta 2O_2^{3-}$] tetrahedra was evidenced due to the presence of the 680, 395 and 350 cm^{-1} bands in Raman spectra of borate glasses [58]. But, in the bismuth containing Raman spectra the Raman signals at 395 and at 350 cm^{-1} are not evidenced. Hence, we cannot readily assign the 680 cm^{-1} Raman signal for $B\Theta_2O_2^{3-}$ tetrahedra.

3.3. Optical Absorption Study

The absorption characteristics of the Eu^{3+} ion in the PbO and Bi_2O_3 lanthanum borate glasses were measured in the UV–Vis region and the resulted spectra is shown in Fig. 3 (a) and (b) respectively. The LPb50Eu*x* and LBi50BEu*x* glasses are exhibited strong UV absorption and good transmission for visible radiation. In both the spectra, 0.5 mol% of Eu^{3+}–doped glass is exhibit a single absorption due to $^7F_0 \rightarrow {}^5D_2$ transition at 464 nm [59]. An additional absorption peak at 393 nm corresponding to $^7F_0 \rightarrow {}^5L_6$ transition appeared in the

lead containing samples for higher Eu^{3+} concentration [59]. The absorption intensity of absorption peaks are increased with Eu^{3+} content and highest for 2 mol % doped glasses. From Fig. 3 it can be seen that among different characteristic absorption peaks of Eu^{3+}, most of absorption bands of Eu^{3+} ion in the UV and visible region are masked due to strong absorption of the host glass [24]. The presence of heavy metal cations such as Pb^{2+} and Bi^{3+} in LPb50BEu*x* and LBi50BEu*x* glasses respectively might be responsible for the strong absorption of the glasses. The increase of Eu^{3+} concentration in the glass resulted in shift in the band edge of the glass from 390 nm to longer wavelength side in the spectrum. This significant change infers, dopant Eu^{3+} ion is playing a network modifier role in the glass network.

The band gap of the glass is related to the variation in the glass structure. Usually band gap of the glass shifts to higher wavelength side due to locally created energy levels near the band edge. Therefore, in the present investigation the band gap of the glasses is determined using Davis and Mott relation [36] which is derived from absorption edge given by

$$\alpha h\upsilon = B(h\upsilon - E_g)^n \quad (1)$$

where *B* is the constant called as band tailing factor, E_g is the optical band gap between the valence band and conduction band, $h\upsilon$ is the photon energy of the incident radiation and *n* is an index of phonon assisted direct and indirect allowed transition equal to ½ and 2 respectively. The Tauc's plots used to estimate the optical bandgap of glasses using aforementioned equation are shown in Fig. 4 and 5. Fig. 4 (a) and 5 (a) represent the plots for direct bandgap measurement for LPb50Eu*x* and LBi50BEu*x* glasses respectively and Fig. 4 (b) and 5 (b) represents the plots for indirect bandgap measurements for LPb50BEu*x* and LBi50BEu*x* glasses respectively. By extrapolating the linear part of $\alpha h\upsilon \; vs \; h\upsilon$ curve is intersected at different values of E ($h\upsilon$) axis. The direct band gap values of glasses after Eu^{3+}

doping are listed in Table 1. The band gap for PbO borate glass is higher than Bi_2O_3 contain glasses and values are decreased with respect to Eu^{3+} doping concentrations. This is also evident from red shift in the absorption edge of the glasses. The newly formed localized energy levels near the absorption edge of the glass helps in electron migration to conduction and decreased the forbidden energy gap. This change is attributed to formation of NBOs in the glass network. The entry of higher atomic radii Eu^{3+} ion ruptured the B–O, Pb–O and Bi–O covalent bond corresponding to different functional groups of the glass network. The doping decreased the number of bridging oxygen's (BOs) O^- in the network and thereby increased the highly polarisable NBOs [38].

3.4. Photoluminescence Properties

The heavy metal borate glass is transparent to optical radiation in the Visible to near infrared (NIR) region. But, the RE doped glass is optically active and exhibits strong absorption and luminescence in the visible to NIR region of electromagnetic spectrum [1]. This versatile behaviour attributed to intra-band 4*f*–4*f* and 4*f*–5*d* electronic transition of triply ionized RE ions [59]. In the PL phenomenon, light is used to excite the RE ions to record the resultant emission (spectrum). The peak position and emission intensity of the Eu^{3+} ion rely on the host glass chemical composition and its concentration. Thus, in the present study, excitation spectra of the Eu^{3+} in the PbO and Bi_2O_3 containing lanthanum borate glasses are recorded by monitoring the emission at 613 nm. Fig. 6 (a) and (b) shows the recorded PL excitation spectra of the LPb50BEu*x* and LBi50BEu*x* glasses respectively. The excitation spectra in both glass hosts shows several peaks, the observed peaks are assigned as shown in the Fig. 6 using the references [60,61]. The intensity of the excitation peaks are enhanced as Eu^{3+} doping increased in PbO containing glasses while the Bi_2O_3 comprising glass host demonstrated the concentration dependency. The excitation peaks at 393 nm and 464 nm is equally high intense among other transitions in the PbO contained glasses. But, in bismuth

contained glasses, excitation peak at 464 nm is highest compared to 393 nm. Thus, the PL spectra of the glass hosts were recorded at both 393 nm and at 464 nm excitations to demonstrate the studied glasses for lighting applications more potentially and their suitability.

The PL emission spectra of LP50BEu*x* and LBi50BEu*x* glass hosts at excitation of 393 nm are shown in Fig. 7 (a) and (b) respectively and the corresponding PL spectra at 464 excitation are depicted in Fig. 7 (c) and (d) for lead and bismuth containing glasses. The Eu^{3+} ion exhibited its characteristic emission wavelengths in visible region of spectrum in both hosts. The emission peaks at 580, 590, 613, 646 and 702 nm are assigned to $^5D_0 \rightarrow {}^7F_0$, $^5D_0 \rightarrow {}^7F_1$, $^5D_0 \rightarrow {}^7F_2$, $^5D_0 \rightarrow {}^7F_3$, $^5D_0 \rightarrow {}^7F_4$ electric and magnetic dipole transitions of the Eu^{3+} ion allowed by $\Delta J = 2$ and 1 selection rules. The band at 613 nm is peaked highest among other transitions. Interestingly, emission at 704 nm is considerably intense compared to band at 591 nm and other heavy metal borate host glasses [52,60]. The Eu^{3+} ion emission intensity of PbO hosted borate glass is dependent on ion concentration and independent to the excitation wavelengths. Whereas, the bismuthate glasses emission shown concentration dependency and intensity quenched at 2 mol % Eu^{3+} doping. Thus, emission intensity is highest at the excitation of 464 nm compared to 393 nm in the LBi50BEu*x* glasses. In LPb50BEu*x* glasses, the luminescence intensity significantly increased at 1 mol % compared to 0.5 mol % of Eu^{3+} and intensity further slightly increased for 2 mol% of Eu^{3+} ions. But in the case of LBi50BEu*x* glasses, emission intensity for Eu^{3+} at 1 mol% enhanced noticeably compared to 0.5 and at 2 mol% Eu^{3+} the bismuth containing glasses exhibited decrease in PL intensity due to concentration quenching. The overall emission intensity of lead and bismuth containing glasses shown in Fig. 7 clearly proves composition dependency of luminescence properties of Eu^{3+} ion. Further, it has been reported that the intensity of 704 nm transition of Eu^{3+} was enhanced greatly along with 613 transition due to high polarizability of the glasses [62]. In the Fig. 7 it can clearly identified that with increase in Eu_2O_3 content in the glasses,

703 nm transition of Eu^{3+} is improved along with 613 transition (not at equal rate) which is attributed to the high polarizability of the studied glasses attained due to the highly polarizable PbO and Bi_2O_3 oxides. PL emission intensity ratio's (R) of orange to red band (electric to magnetic dipole transition) infers local asymmetry around the Eu^{3+} ion offered by surrounding ligands and it also infer the chemical bond strengths of Eu–O [60]. The calculated intensity ratio (R) values at the excitation of 393 nm and 464 nm are provided in Table 2 and 3 respectively. The R values are highest for LPb50BEu*x* glass over LBi50BEu*x* glasses suggests Eu^{3+} ion centered at highly asymmetric site and possess higher Eu–O covalence in the PbO framed borate glass network compared to Bi_2O_3 framed borate glass [63]. Nonetheless, the R values higher than the unity for all the investigated glass samples suggest the Eu^{3+} ions are situated in acentric sites [62].

The Judd–Ofelt (JO) [64,65] theory access the quantitative luminescence properties such as branching ratio, radiation transition probability, emission cross-section and total radiative lifetime of Eu^{3+} ions in the given host [66,67]. The JO intensity parameters of the host medium used to predict the above mentioned radiative properties of the prepared glasses. The JO parameters related to LPb50BEu*x* and LBi50BEu*x* glasses were calculated using emission spectrum and using corresponding relations mentioned in reference [36]. The JO parameters, Ω_2 varies according to the strength of Eu–O covalence and short range structural rearrangement around the Eu^{3+} ion, where as Ω_4 and Ω_6 parameters are attributed to the glass rigidity and viscosity [68]. The calculated values of JO parameters at the excitation of 393 nm and at 464 nm are furnished in Table 2 and 3 respectively. Since the PL intensity and JO parameters are better at 464 nm excitation and hence the JO parameters (obtained at excitation of 464 nm) are compared with other heavy metal borate glasses [22,36,63,69,70]. The value Ω_2 and Ω_4 of LPb50BEu*x* glasses are more compared to LBi50BEu*x* glass shows

strength of covalent bonding of Eu^{3+} to O^- in PbO framed B_2O_3 glass network is much higher.

The lasing properties of the investigated glasses calculated using JO parameters with the relations found in previously mentioned reference. The calculated radiative parameters of the LPb50BEu*x* and LBi50BEu*x* glass are listed in Table 4 and 5 respectively for 393 and 464 nm excitations. The deciding factor for lasing transition such as branching ratio is should be more than 0.5 for given emission transition. Among all emission peaks, $^7F_0 \rightarrow {}^5D_2$ transition of Eu^{3+} ion is exhibited such potentiality and both the glass host containing 1 mol % of Eu^{3+} yielded highest branching ratio compared to other prepared glasses. The RE doped glass is useful as optical gain material for solid state laser and it is dependent on stimulated emission cross–section of particular transition [71,72]. Interestingly, $^5D_0 \rightarrow {}^7F_4$ transition has gain slightly large stimulated cross–section compared to $^5D_0 \rightarrow {}^7F_2$ emission band. But, this transition has shortage of required branching ratio to achieve necessary population inversion. The reciprocal of the total transition probability gives metastable life of excited state $^5D_0$ state and calculated values decreased as increase in number density of Eu^{3+} ion in the glass network. The actual lifetime of metastable state and quantum efficiency can be determined by decay curve analysis. The recoded curves of optimized glass samples i.e. LPb50BEu1 and LBi50BEu1 glasses were measured at the excitation of 464 nm and are shown in Fig. 8. The single exponential function is well fitted to observed decay curves [36]. The obtained lifetime of $^5D_0$ state is 1.29 ms and 1.01 ms for PbO and Bi_2O_3 comprising glasses respectively. The LPb50BEu1 and LBi50BEu1 glasses has gained optimum stimulated emission cross–section and optical gain values for $^5D_0 \rightarrow {}^7F_2$ transition at 613 nm compared to other studied glasses, suggesting that the heavy metal borate glasses containing 1 mol % of Eu^{3+} are potential photonic materials. Further, obtained quantum efficiency (τ_{mea}/τ_{cal}) of the lead containing glass is 85 % compared with 50 % of bismuth hosted glass signifies

LPb50BEu1 glass is most luminescent material compared to other borate network glasses [36]. The quantum efficiency values of the investigated glasses are considerably higher compared to other borate glasses reported recently [36].

4. Conclusion

The varied concentration of Eu^{3+} ions activated heavy metal borate glasses were fabricated and the effect of Eu^{3+} ions on optical absorption, optical band gap and PL properties were analysed. The XRD profiles were confirmed the glassy nature of prepared glasses. The optical band gap values were demonstrated decreasing trend with increase in Eu_2O_3 concertation due to the decrease of bridging oxygen's over non-bridging oxygen's (NBO's). These NBO's in the glass network provides more scope for light–matter interaction through its less bounded excited electrons. The PL emission properties were analysed under UV and blue light excitations. The PL intensity was increased with increase in Eu^{3+} content in lead containing glass samples whereas it was decreased at 2 mol % of Eu^{3+} in bismuth framed glasses. The JO parameters and radiative properties clearly suggest the investigated glasses containing 1 mol % of Eu^{3+} were competing materials for red light solid state lighting application under blue light excitations. Further, the life time and quantum efficiency values of lead containing glass significantly high compared to bismuth containing borate glass. Therefore, the PbO framed borate glass host is more precisely suitable than Bi_2O_3 containing borate glass for solid state lighting applications under blue light excitations.

Acknowledgements

The Authors PR and MKK would like to thank DST–FIST for providing XRD measurements at Department of Physics, Bangalore University, Bangalore. The Authors PR

and GJ thankful to Dr. Amarnath R Allu, Scientist CSIR–CGCRI, Kolkata for life time measurements and valuable suggestions. The Authors PR and GJ grateful to Dr. Subrata Das, Senior Scientist, NIIST, Thiruvananthapuram for providing PL measurements. The authors PR and GJ are thankful to Dr. Sudipta Som, Department of Chemical Engineering, National Taiwan University, Taiwan for useful discussions and suggestions. One of the authors (PR) is thankful to late Dr. Rajan V Anavekar, Former Professor, Department of Physics, Bangalore University, Bangalore, for useful discussions and valuable suggestions.

References:

[1] A.S. Kuznetsov, V.K. Tikhomirov, M. V. Shestakov, V. V. Moshchalkov, Nanoscale 5 (2013) 10065–10075.

[2] K. Linganna, R. Narro-García, H. Desirena, E. De La Rosa, C. Basavapoornima, V. Venkatramu, C.K. Jayasankar, J. Alloys Compd. 684 (2016) 322–327.

[3] K. Haladejová, A. Prnová, R. Klement, W.H. Tuan, S.J. Shih, D. Galusek, J. Eur. Ceram. Soc. 36 (2016) 2969–2973.

[4] G. Ji, G. joon Hong, C. hyuck Bae, P. Babu, K.S. Lim, Appl. Surf. Sci. 478 (2019) 412–416.

[5] F. Steudel, S. Loos, B. Ahrens, S. Schweizer, J. Lumin. 170 (2016) 770–777.

[6] F. Zaman, J. Kaewkhao, G. Rooh, N. Srisittipokakun, H.J. Kim, J. Alloys Compd. 676 (2016) 275–285.

[7] X. Zhang, L. Huang, F. Pan, M. Wu, J. Wang, Y. Chen, Q. Su, ACS Appl. Mater. Interfaces 6 (2014) 2709–2717.

[8] X. Zhang, J. Wang, L. Huang, F. Pan, Y. Chen, B. Lei, M. Peng, M. Wu, ACS Appl. Mater. Interfaces 7 (2015) 10044–10054.

[9] S. Tabanli, G. Eryurek, Sensors Actuators, A Phys. 285 (2019) 448–455.

[10] J.S. Zhong, H.B. Gao, Y.J. Yuan, L.F. Chen, D.Q. Chen, Z.G. Ji, J. Alloys Compd. 735 (2018) 2303–2310.

[11] P. Zheng, S. Li, L. Wang, T.-L. Zhou, S. You, T. Takeda, N. Hirosaki, R.-J. Xie, ACS Appl. Mater. Interfaces 10 (2018) 14930–14940.

[12] P. Cai, X. Wang, H.J. Seo, Phys. Chem. Chem. Phys. 20 (2018) 2028–2035.

[13] M. Gong, Q. Liu, B. Cook, B. Kattel, T. Wang, W.-L. Chan, D. Ewing, M. Casper, A. Stramel, J.Z. Wu, ACS Nano 11 (2017) 4114–4123.

[14] X. Wang, Y. Wang, Y. Bu, X. Yan, J. Wang, P. Cai, T. Vu, H.J. Seo, Sci. Rep. 7 (2017).

[15] X. Chen, W. Xu, L. Zhang, X. Bai, S. Cui, D. Zhou, Z. Yin, H. Song, D.-H. Kim, Adv. Funct. Mater. 25 (2015) 5462–5471.

[16] D.F. Franco, A.C. Sant'Ana, L.F.C. De Oliveira, M.A.P. Silva, J. Mater. Chem. C 3 (2015) 3803–3808.

[17] T.A. Lodi, N.F. Dantas, T.S. Gonçalves, A.S.S. de Camargo, F. Pedrochi, A. Steimacher, J. Lumin. 207 (2019) 378–385.

[18] V. Hegde, C.S.D. Viswanath, K.K. Mahato, S.D. Kamath, Mater. Chem. Phys. 234 (2019) 369–377.

[19] A.U. Trápala-Ramírez, J.L.N. Gálvez-Sandoval, A. Lira, I. Camarillo, E. Alvarez-Ramos, A.N. Meza-Rocha, U. Caldiño, J. Lumin. 215 (2019).

[20] S. Selvi, K. Marimuthu, G. Muralidharan, J. Non. Cryst. Solids 461 (2017) 35–46.

[21] W.A. Pisarski, T. Goryczka, J. Pisarska, W. Ryba-Romanowski, J. Phys. Chem. B 111 (2007) 2427–2430.

[22] S. Pravinraj, M. Vijayakumar, K. Marimuthu, Phys. B Condens. Matter 509 (2017) 84–93.

[23] X. Huang, S. Han, W. Huang, X. Liu, Chem. Soc. Rev. 42 (2013) 173–201.

[24] B.C. Jamalaiah, L.R. Moorthy, H.J. Seo, J. Non. Cryst. Solids 358 (2012) 204–209.

[25] Y. Wang, J. Cao, X. Li, J. Li, L. Tan, S. Xu, M. Peng, J. Am. Ceram. Soc. (2018) jace.16067.

[26] K. Ouannes, K. Lebbou, B.M. Walsh, M. Poulain, G. Alombert-Goget, Y. Guyot, J. Alloys Compd. 649 (2015) 564–572.

[27] C. Doerenkamp, E. Carvajal, C.J. Magon, W.J.G.J. Faria, J.P. Donoso, Y. Galvão Gobato, A.S.S. de Camargo, H. Eckert, J. Phys. Chem. C 123 (2019) 22478–22490.

[28] M. Haouari, F. Ben Slimen, A. Maaoui, N. Gaumer, J. Alloys Compd. 743 (2018) 586–596.

[29] G. Gao, J. Wei, Y. Shen, M. Peng, L. Wondraczek, J. Mater. Chem. C 2 (2014) 8678–8682.

[30] H. Wen, G. Jia, C.K. Duan, P.A. Tanner, Phys. Chem. Chem. Phys. 12 (2010) 9933–9937.

[31] Hirdesh, A. Khanna, J. Lumin. 204 (2018) 319–326.

[32] C. Yu, Z. Yang, J. Qiu, Z. Song, Z. Dacheng, J. Am. Ceram. Soc. 101 (2018) 612–623.

[33] I. Burmistrov, D. Agarkov, I. Tartakovskii, V. Kharton, S. Bredikhin, ECS Trans. 68 (2015) 1265–1274.

[34] D.A. Agarkov, I.N. Burmistrov, F.M. Tsybrov, I.I. Tartakovskii, V. V. Kharton, S.I. Bredikhin, Russ. J. Electrochem. 52 (2016) 600–605.

[35] D.A. Agarkov, I.N. Burmistrov, F.M. Tsybrov, I.I. Tartakovskii, V. V. Kharton, S.I. Bredikhin, Solid State Ionics 302 (2017) 133–137.

[36] V. Hegde, C.S.D. Viswanath, V. Upadhyaya, K.K. Mahato, S.D. Kamath, Phys. B Condens. Matter 527 (2017) 35–43.

[37] G. Jagannath, B. Eraiah, K. NagaKrishnakanth, S. Venugopal Rao, J. Non. Cryst. Solids 482 (2018) 160–169.

[38] G. Upender, S. Ramesh, M. Prasad, V.G. Sathe, V.C. Mouli, J. Alloys Compd. 504 (2010) 468–474.

[39] Y.G. Choi, K.H. Kim, V.A. Chernov, J. Heo, J. Non. Cryst. Solids 259 (1999) 205–211.

[40] P. Limkitjaroenporn, J. Kaewkhao, P. Limsuwan, W. Chewpraditkul, J. Phys. Chem. Solids 72 (2011) 245–251.

[41] E.I. Kamitsos, M.A. Karakassides, G.D. Chryssikos, J. Phys. Chem. 91 (1987) 1073–1079.

[42] B.V.R. Chowdari, Z. Rong, Solid State Ionics 90 (1996) 151–160.

[43] E.I. Kamitsos, A.P. Patsis, M.A. Karakassides, G.D. Chryssikos, J. Non. Cryst. Solids 126 (1990) 52–67.

[44] I. Kashif, A. Abd El-Maboud, R. El-Said, E.M. Sakr, A.A. Soliman, J. Alloys Compd. 539 (2012) 124–128.

[45] Y. Cheng, H. Xiao, W. Guo, W. Guo, Thermochim. Acta 444 (2006) 173–178.

[46] Y.B. Saddeek, M.S. Gaafar, Mater. Chem. Phys. 115 (2009) 280–286.

[47] Y.B. Saddeek, M.S. Gaafar, S.A. Bashier, J. Non. Cryst. Solids 356 (2010) 1089–1095.

[48] Y. Cheng, H. Xiao, W. Guo, W. Guo, Ceram. Int. 33 (2007) 1341–1347.

[49] D. Maniua, T. Iliescu, I. Ardelean, S. Cinta-Pinzaru, N. Tarcea, W. Kiefer, in: J. Mol. Struct., Elsevier, 2003, pp. 485–488.

[50] B.N. Meera, A.K. Sood, N. Chandrabhas, J. Ramakrishna, J. Non. Cryst. Solids 126 (1990) 224–230.

[51] H.A. Othman, A. Herrmann, D. Möncke, Int. J. Appl. Glas. Sci. 10 (2019) 339–348.

[52] B. Shanmugavelu, V.V.R.K. Kumar, R. Kuladeep, D.N. Rao, J. Appl. Phys. 114 (2013).

[53] W.L. Konijnendijk, J.M. Stevels, J. Non. Cryst. Solids 18 (1975) 307–331.

[54] B.N. Meera, J. Ramakrishna, J. Non. Cryst. Solids 159 (1993) 1–21.

[55] Z.Y. Yao, D. Möncke, E.I. Kamitsos, P. Houizot, F. Célarié, T. Rouxel, L. Wondraczek, J. Non. Cryst. Solids 435 (2016) 55–68.

[56] M. Dogra, K.J. Singh, K. Kaur, V. Anand, P. Kaur, P. Singh, B.S. Bajwa, Radiat. Phys. Chem. 144 (2018) 171–179.

[57] K. Chen, L. Fang, T. Zhang, S.P. Jiang, J. Mater. Chem. A 2 (2014) 18655–18665.

[58] E.I. Kamitsos, G.D. Chryssikos, J. Mol. Struct. 247 (1991) 1–16.

[59] W.T. Carnall, P.R. Fields, K. Rajnak, J. Chem. Phys. 49 (1968) 4424–4442.

[60] S. Balaji, P. Abdul Azeem, R.R. Reddy, Phys. B Condens. Matter 394 (2007) 62–68.

[61] C.S. Dwaraka Viswanath, K. Venkata Krishnaiah, C.K. Jayasankar, Opt. Mater. (Amst). 83 (2018) 348–355.

[62] G. Jagannath, B. Eraiah, K. Jayanthi, S.R. Keshri, S. Som, G. Vinitha, A.G. Pramod, K.N. Krishnakanth, G. Devarajulu, S. Balaji, S. Venugopal Rao, K. Annapurna, S. Das, A.R. Allu, Phys. Chem. Chem. Phys. (2020).

[63] K. Swapna, S. Mahamuda, A.S. Rao, T. Sasikala, P. Packiyaraj, L.R. Moorthy, G.V. Prakash, J. Lumin. 156 (2014) 80–86.

[64] B.R. Judd, Phys. Rev. 127 (1962) 750–761.

[65] G.S. Ofelt, J. Chem. Phys. 37 (1962) 511–520.

[66] B.R. Judd, J. Math. Phys. 3 (1962) 557–563.

[67] G.S. Ofelt, J. Chem. Phys. 38 (1963) 2171–2180.

[68] C.B. Annapurna Devi, S. Mahamuda, K. Swapna, M. Venkateswarlu, A. Srinivasa Rao, G. Vijaya Prakash, Opt. Mater. (Amst). 73 (2017) 260–267.

[69] B.C. Jamalaiah, J.S. Kumar, A.M. Babu, L.R. Moorthy, J. Alloys Compd. 478 (2009) 63–67.

[70] S. Selvi, K. Marimuthu, N. Suriya Murthy, G. Muralidharan, J. Mol. Struct. 1119 (2016) 276–285.

[71] C. Görller-Walrand, K.B.- North-Holland, undefined Amsterdam, undefined 1998, (n.d.).

[72] P. Paufler, Cryst. Res. Technol. 30 (1995) 926–926.

List of Tables with their Captions

Table 1: Physical properties of the un-doped and Eu^{3+}doped PbO and Bi_2O_3 lanthanum borate glasses.

Properties (± error limits)	**LPb50B**	**LPb50Eu0.5**	**LPb50BEu1**	**LPb50BEu2**	**LBi50B**	**LBi50Eu0.5**	**LBi50 Eu1**	**LBi50 Eu2**
Physical Properties								
Average Molecular Weight, M ($gmol^{-1}$)	156.67	158.08	159.49	162.32	293.41	294.82	296.233	299.056
Density, ρ (gcm^{-3})(±0.002)	5.393	5.36	5.103	5.043	6.812	6.795	5.808	5.940
Molar Volume, V_m (cm^3mol^{-1})(±0.001)	29.05	29.45	31.25	32.18	43.071	43.387	50.996	50.339
Refractive index, n(±0.001)	1.79	1.80	1.81	1.83	2.084	2.089	2.142	2.171
Dielectric constant, ϵ(±0.001)	3.23	3.24	3.28	3.37	4.343	4.363	4.588	4.713
Molar Refractivity, R_M (cm^{-3})(±0.002)	12.40	12.60	13.50	14.20	22.700	22.934	27.774	27.843
Electronic Polarizability, α_e($\times 10^{-24}$ cm^3)(±0.001)	4.91	4.99	5.35	5.63	8.996	9.089	11.00	11.03
Optical Properties								
Direct optical band gap, E_g^{dir} (eV) (±0.002)	2.812	2.866	2.770	2.634	2.623	2.551	2.515	2.325
Indirect band gap, E_g^{indir}	2.300	2.575	2.439	2.188	2.373	2.314	2.268	2.136

(eV) (±0.002)								
Inter- ionic Properties								
Concentration of Eu2O3 (mol %)	0	0.5	1	2	0	0.5	1	2
Eu^{3+} concentration, N ($\times 10^{22}$ions/cm^3) (±0.0001)	-	1.92	1.022	3.74	-	0.694	1.181	2.392
Eu-Eu Interionic spacing, d_{Eu-Eu} (Å) (±0.0001)	-	4.68	3.79	3.04	-	5.331	4.466	3.041

Table 2: JO parameters Ω_2 and Ω_4 (x 10^{-20}) and Intensity ratio (R) values of Eu_2O_3 doped glasses at the excitation of 393 nm

Glass Code	Ω_2	Ω_4	R	References
LPb50BEu0.5	3.30	4.20	2.61	Present work
LPb50BEu1	4.73	4.48	3.75	Present work
LPb50BEu2	4.22	4.03	3.35	Present work
LBi50BEu0.5	3.02	5.15	2.4	Present work
LBi50BEu1	3.95	4.66	3.12	Present work
LBi50BEu2	3.94	4.83	3.14	Present work

Table 3: JO parameters Ω_2 and Ω_4 (x 10^{-20}) and Intensity ratio (R) values of Eu_2O_3 doped glasses at 464 nm

Glass Code	Ω_2	Ω_4	R	References
LPb50BEu0.5	4.69	5.15	8.75	Present work
LPb50BEu1	6.86	6.75	5.45	Present work
LPb50BEu2	5.98	6.87	4.75	Present work
LBi50BEu0.5	3.55	4.46	2	Present work
LBi50BEu1	5.33	4.6	4.23	Present work
LBi50BEu2	5.57	4.96	4.2	Present work
BTPAE	3.53	5.54	1.08	[22]
ZnAlBiB	2.19	1.49	2.66	[63]
ZNBBE	5.14	4.17	3.98	[36]
LBTAF	4.71	0.48	4.77	[69]
LBTPE	3.12	3.12	0.08	[70]

Table 4: Emission peak wavelength (λ_p, nm), effective bandwidth ($\Delta\lambda_p$, *nm*), Radiative transition probabilities (A, s^{-1}), Total radiative transition probabilities (A_T, s^{-1}), stimulated emission cross section ($\sigma_{se}\ x\ 10^{-22}\ cm^2$), experimental branching ratios (β_{exp}), gain band width ($\sigma_{se}\ x\ \Delta\lambda_p$) ($x\ 10^{-28}$, cm^3) of the Eu_2O_3-doped glasses at the excitation of 393 nm.

Transitions $^5D_0\rightarrow$	Parameters	LPb50BEu0.5	LPb50BEu1	LPb50BEu2	LBi50BEu0.5	LBi50BEu1	LBi50BEu2
$^7F_1$	λ_p	592	592	592	592	592	592
	$\Delta\lambda_p$	13	15.1	15.1	12.9	14.2	12.9
	A	73.11	73.11	73.11	73.11	73.11	73.11
	σ_{se}	2.73	2.35	2.35	2.35	2.36	2.36
	β_R	0.18	0.15	0.16	0.16	0.16	0.16
	$\sigma_{se}\ x\ \Delta\lambda_p$	3.54	3.54	3.54	3.03	3.35	3.04
$^7F_2$	λ_p	612	612	612	612	612	612
	$\Delta\lambda_p$	13	14	14	12.7	12.9	12.8
	A	195	280	250	233	234	234
	σ_{se}	8.33	11.1	9.90	7.63	9.97	10.8
	β_R	0.50	0.58	0.57	0.52	0.53	0.53
	$\sigma_{se}\ x\ \Delta\lambda_p$	10.8	15.54	13.86	9.69	12.86	13.82
$^7F_4$	λ_p	704	704	704	704	704	704
	$\Delta\lambda_p$	10	11.33	11.7	10.1	12	10.2
	A	118	126	113	145	131	136
	σ_{se}	11.4	11.1	9.32	13.9	10.5	13.1
	β_R	0.30	0.26	0.26	0.36	0.29	0.30
	$\sigma_{se}\ x\ \Delta\lambda_p$	11.4	12.54	10.90	14.03	12.6	13.36
	A_T	387	497	436	397	438	442
	τ_{cal}	2.58	2.05	2.28	2.51	2.28	2.22

Table 5: Emission peak wavelength (λ_p, nm), effective bandwidth ($\Delta\lambda_p$, *nm*), Radiative transition probabilities (A, s^{-1}), Total radiative transition probabilities (A_T, s^{-1}), stimulated emission cross section ($\sigma_{se}\ x\ 10^{-22}\ cm^2$), experimental branching ratios (β_{exp}), gain band width ($\sigma_{se}\ x\ \Delta\lambda_p$) ($x\ 10^{-28}$, cm^3) of the Eu_2O_3 doped glasses at the excitation of 464 nm.

Transitions $^5D_0\rightarrow$	Parameters	LPb50BEu0.5	LPb50BEu1	LPb50BEu2	LBi50BEu0.5	LBi50BEu1	LBi50BEu2
	λ_p	592	592	592	592	592	592
$^7F_1$	$\Delta\lambda_p$	15	15.2	15.2	15	15.1	15.1
	A	73.11	73.11	73.11	73.11	73.11	73.11
	σ_{se}	2.33	2.32	2.33	2.36	2.35	2.35
	β_R	0.14	0.10	0.11	0.20	0.14	0.13
	$\sigma_{se}\ x\ \Delta\lambda_p$	3.49	3.59	3.54	3.54	3.54	3.54
	λ_p	612	612	612	612	612	612
	$\Delta\lambda_p$	13.84	13.81	13.80	13.9	13.21	14.07
$^7F_2$	A	277.88	406.45	354.31	151.08	315.11	330.02
	σ_{se}	12.20	14.6	14.2	8.96	14.6	13.52
	β_R	0.55	0.60	0.57	0.43	0.60	0.60
	$\sigma_{se}\ x\ \Delta\lambda_p$	18.3	25.25	24.56	12.45	19.28	19.02
	λ_p	704	704	704	704	704	704
	$\Delta\lambda_p$	11.59	11.59	11.56	9.9	12.04	10.7
$^7F_4$	A	145.31	190.46	193.85	125.84	129.79	139.95
	σ_{se}	12.25	17.6	15.8	11.4	12.7	10.4
	β_R	0.29	0.28	0.31	0.35	0.250	0.257
	$\sigma_{se}\ x\ \Delta\lambda_p$	14.19	20.39	18.26	11.28	15.29	11.12
	A_T	496.314	670.0338	621.2799	350.0494	518.7146	543.0927
	τ_{cal}	2.01 ms	1.49 ms	1.61 ms	2.83 ms	1.94 ms	1.84 ms

Figures Captions:

Figure 1: XRD profiles of prepared LPb50B and LBi50B glasses, and respective glasses containing 1 mol % of Eu_2O_3.

Figure 2: FTIR spectra (a) and Raman spectra (b) of Eu free LPb50B and LBi50B glasses.

Figure 3: Optical absorption spectra of LPb50BEu*x* (a) and LBi50BEu*x* (b) glasses.

Figure 4: Plots of $(\alpha h\nu)^2$ v/s hν (eV) for direct (a), $(\alpha h\nu)^{1/2}$ v/s hν (eV) for indirect (b) bandgap measurements LPb50BEu*x* glasses.

Figure 5: Plots of $(\alpha h\nu)^2$ v/s hν (eV) for direct (a), $(\alpha h\nu)^{1/2}$ v/s hν (eV) for indirect (b) bandgap measurements LBi50BEu*x* glasses.

Figure 6: PL Excitation Spectra of Eu^{3+} doped LPb50BEu*x* (a) and LBi50BEu*x* (b) glasses.

Figure 7: PL emission spectra of LPb50BEu*x* (a) and LBi50BEu*x* (b) glasses at 393 nm excitation. PL emission spectra of LP50BEu*x* (c) and LBi50BEu*x* (d) glasses at the excitation of 464 nm.

Figure 8: The decay curves for $^5D_0 \rightarrow {}^7F_2$ (612 nm) emission of Eu^{3+} ions LPb50BEu1 and LBi50BEu1 glasses when excited at 464 nm.

Credit author statement

P. Ramesh: Carried the materials synthesis, characterization, **Vinod Hegde:** Recorded the absorption spectra**, A.G. Pramod:** Collected the XRD profiles, **B. Eraiah:** Helped in collecting the FTIR spectra, G**. Jagannath:** Completed the JO parameters calculations and analysis, **D.A. Agarkov and G.M. Eliseeva:** Recorded the Raman spectra and contributed in structural analysis, K**. Annapurna:** Contributed to concept discussion and in paper writing. **M.K. Pandey:** Helped in PL analysis, concept discussion and in paper writing. **M.K. Kokila:** Mainly supervised the whole research from content to final analysis

Figure

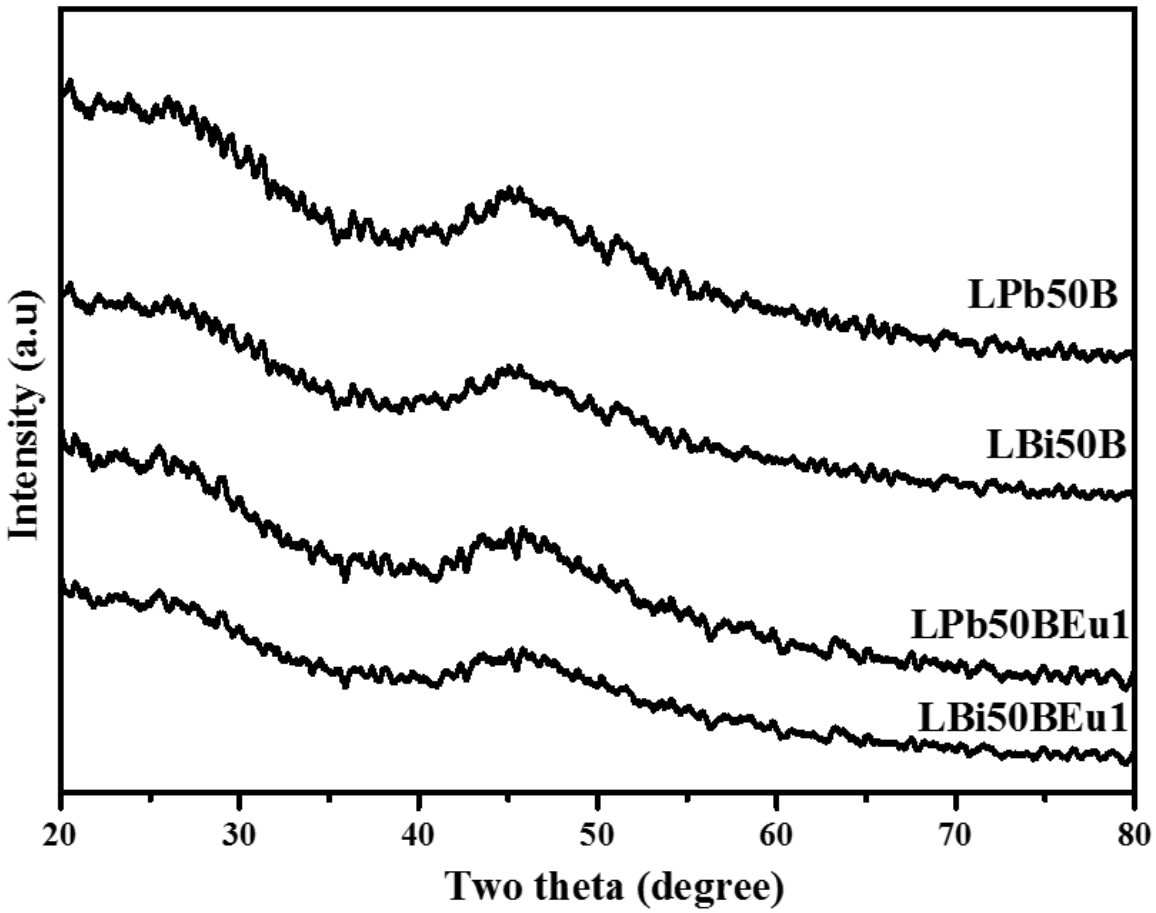

Figure 1:

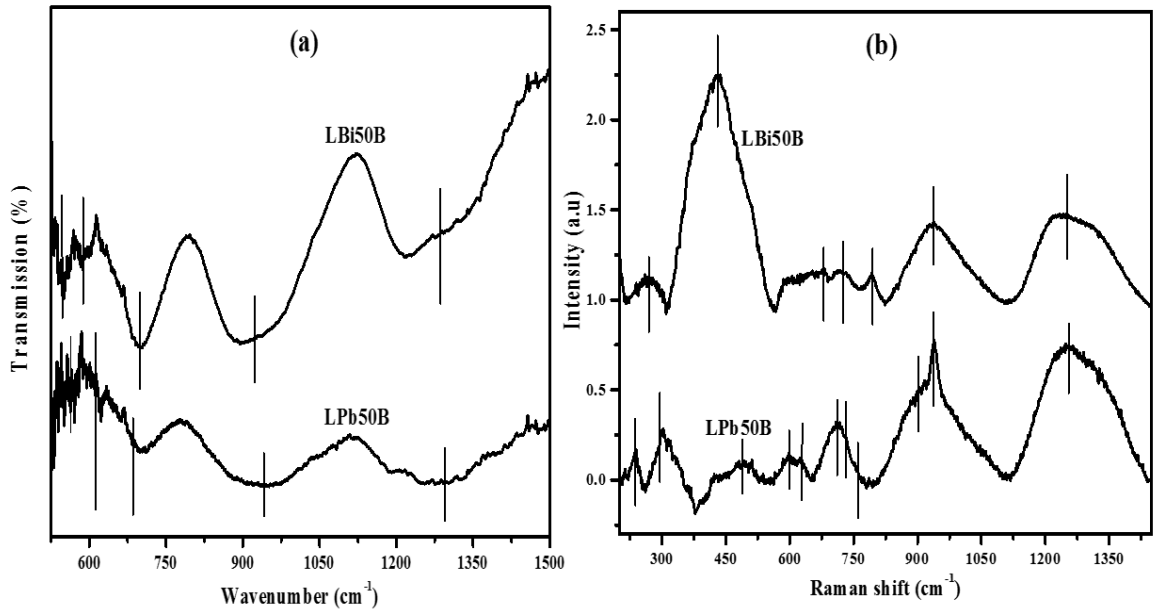
(a)
LBi50B
LPb50B
Transmission (%)
600
750
900
1050
1200
1350
1500
Wavenumber (cm-1)
(b)
LBi50B
LPb50B
Intensity (a.u)
2.5
2.0
1.5
1.0
0.5
0.0
300
450
600
750
900
1050
1200
1350
Raman shift (cm-1)

Figure 2:

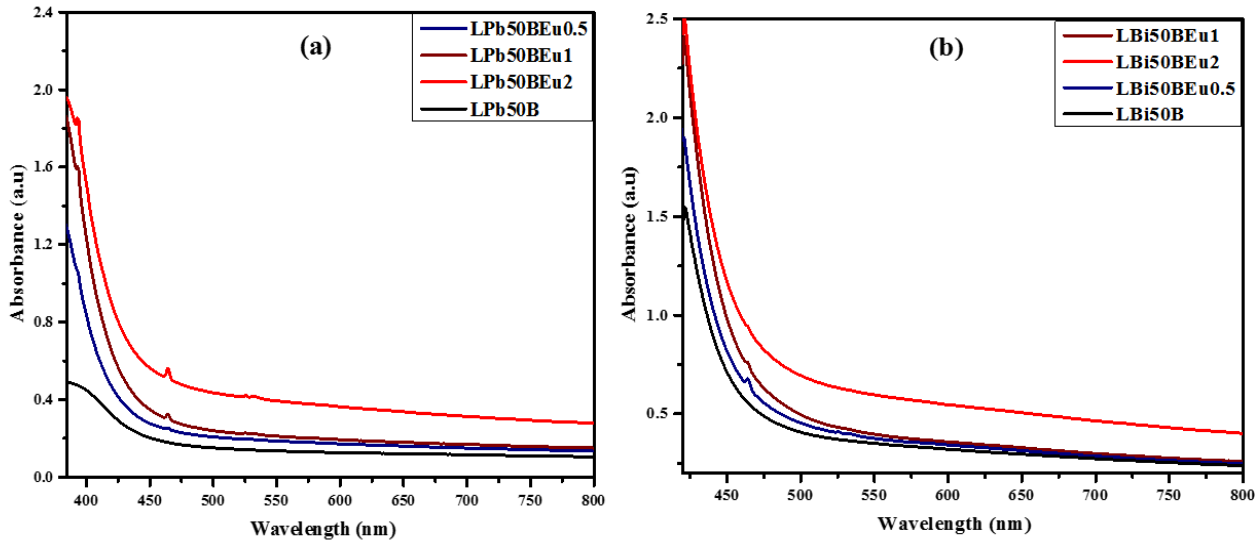
(a)
LPb50BEu0.5
LPb50BEu1
LPb50BEu2
LPb50B
Absorbance (a.u)
Wavelength (nm)
(b)
LBi50BEu1
LBi50BEu2
LBi50BEu0.5
LBi50B
Absorbance (a.u)
Wavelength (nm)

Figure 3:

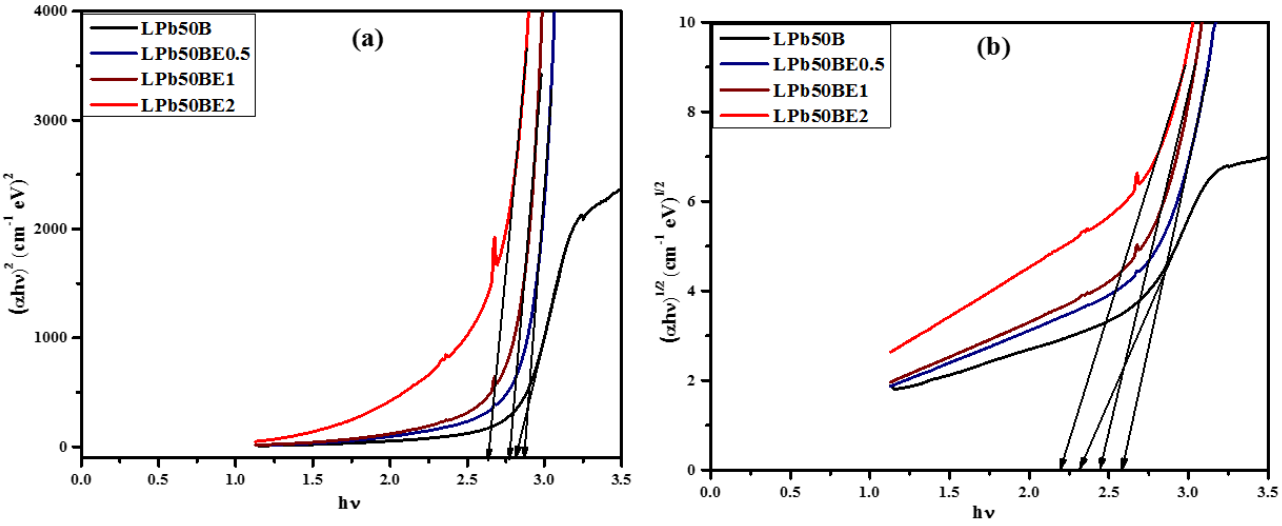
LPb50B
LPb50BE0.5
LPb50BE1
LPb50BE2
(a)
$(\alpha h\nu)^2$ (cm^{-1} eV)^2
hν
(b)
$(\alpha h\nu)^{1/2}$ (cm^{-1} eV)$^{1/2}$

Figure 4:

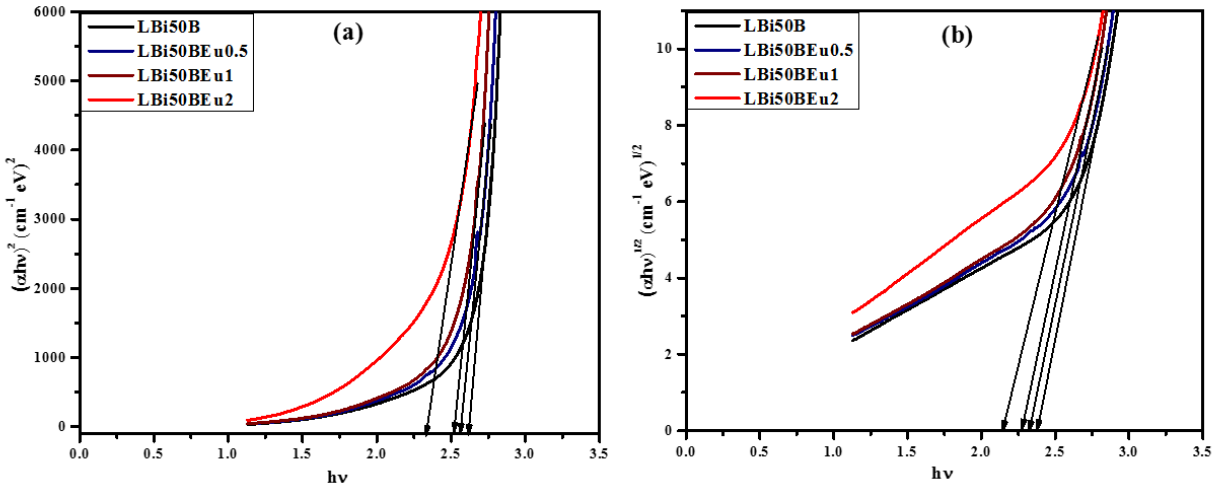
(a)
LBi50B
LBi50BEu0.5
LBi50BEu1
LBi50BEu2
(αhν)² (cm⁻¹ eV)²
hν
(b)
LBi50B
LBi50BEu0.5
LBi50BEu1
LBi50BEu2
(αhν)^1/2 (cm⁻¹ eV)^1/2
hν

Figure 5:

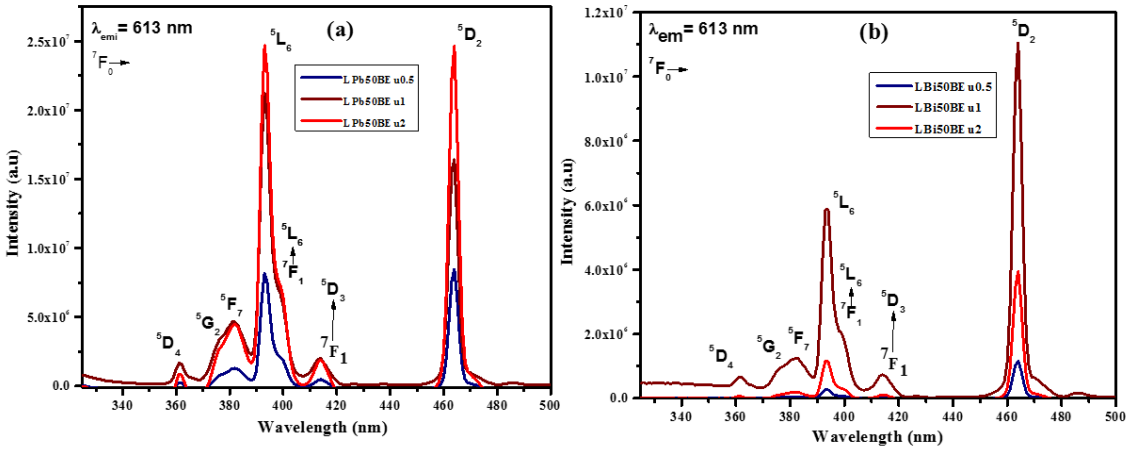
λemi= 613 nm
7F0
(a)
LPb50BE u0.5
LPb50BE u1
LPb50BE u2
5L6
5D2
5L6
7F1
5D3
5D4
5G2
5F7
7F1
Intensity (a.u)
Wavelength (nm)
λem= 613 nm
7F0
(b)
LBi50BE u0.5
LBi50BE u1
LBi50BE u2
5D2
5L6
5L6
7F1
5D3
5D4
5G2
5F7
7F1
Intensity (a.u)
Wavelength (nm)

Figure 6:

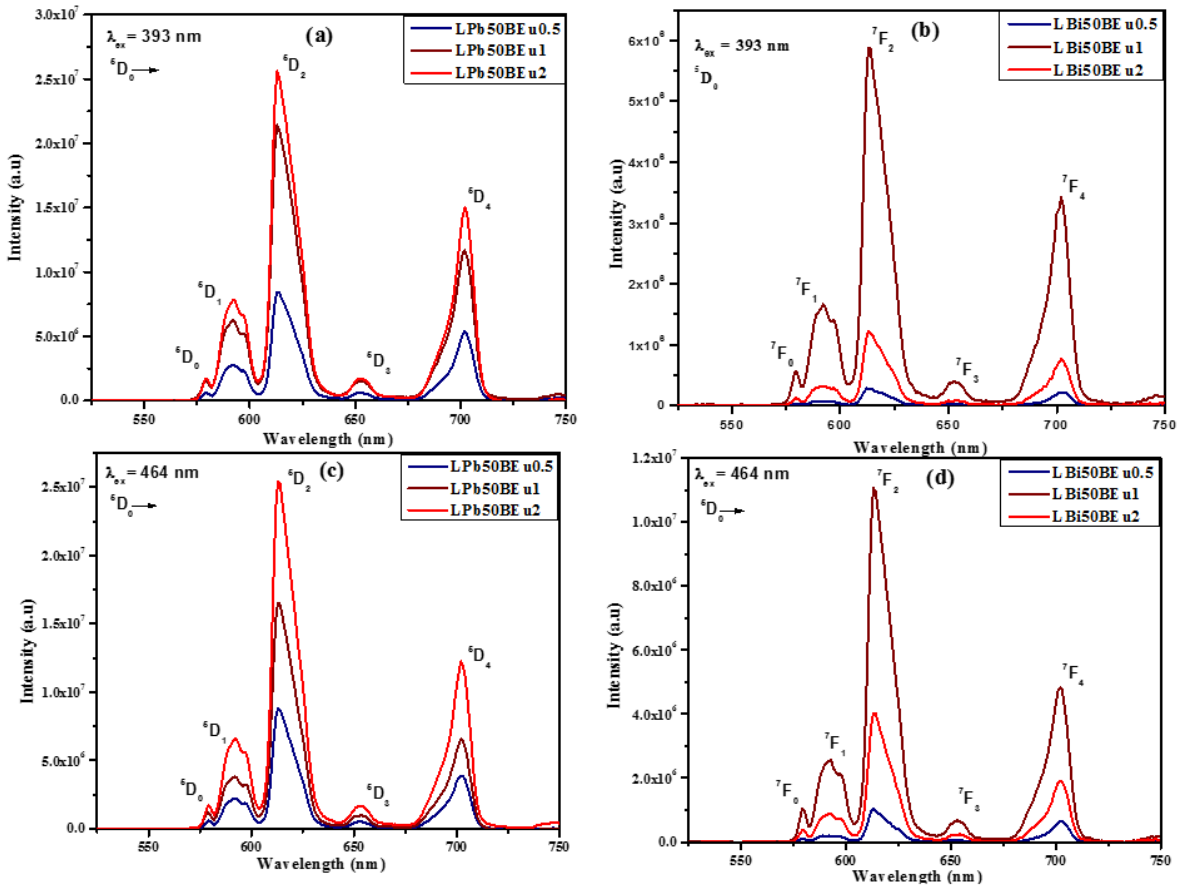
(a)
λex = 393 nm
5D0
LPb50BEu0.5
LPb50BEu1
LPb50BEu2
5D0
5D1
5D2
5D3
5D4
Intensity (a.u)
Wavelength (nm)
(b)
λex = 393 nm
5D0
LBi50BEu0.5
LBi50BEu1
LBi50BEu2
7F0
7F1
7F2
7F3
7F4
Intensity (a.u)
Wavelength (nm)
(c)
λex = 464 nm
5D0
LPb50BEu0.5
LPb50BEu1
LPb50BEu2
5D0
5D1
5D2
5D3
5D4
Intensity (a.u)
Wavelength (nm)
(d)
λex = 464 nm
5D0
LBi50BEu0.5
LBi50BEu1
LBi50BEu2
7F0
7F1
7F2
7F3
7F4
Intensity (a.u)
Wavelength (nm)

Figure 7:

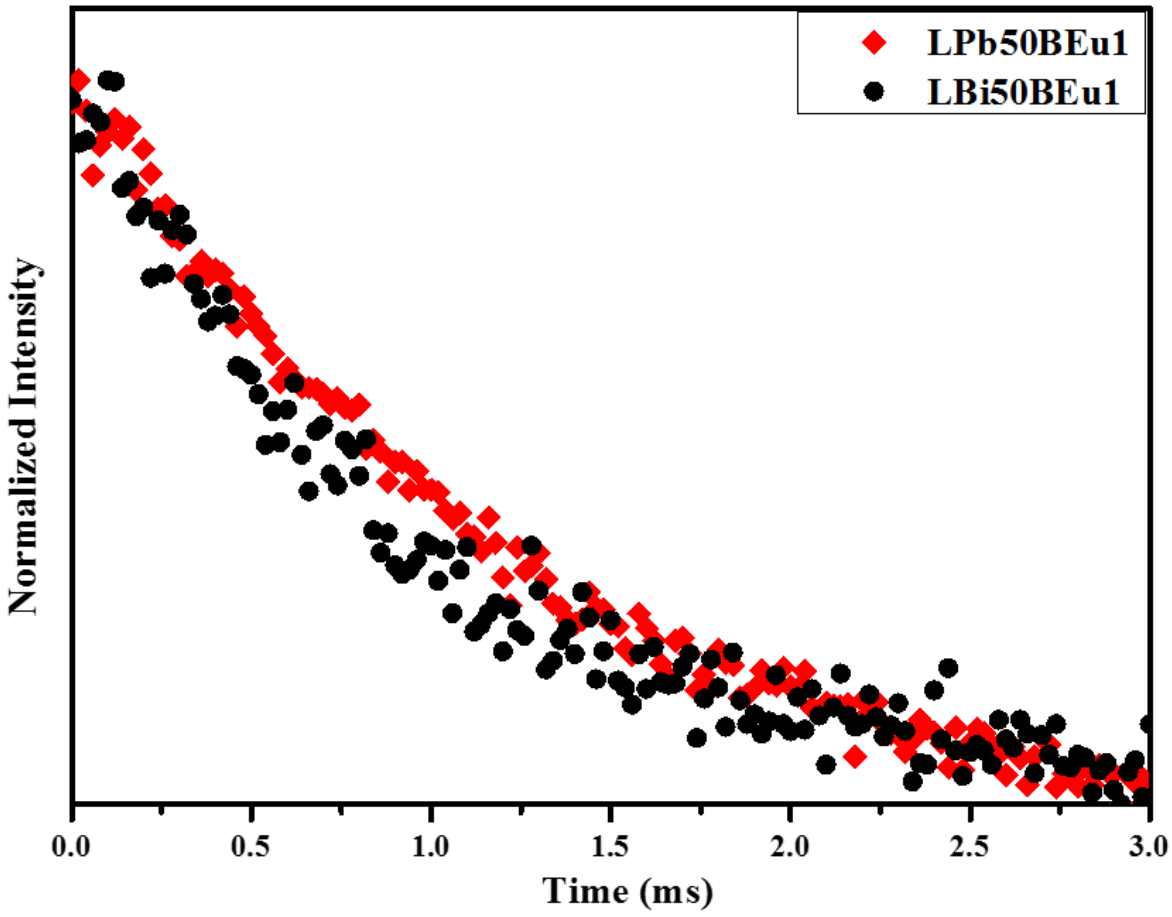
LPb50BEu1
LBi50BEu1
Normalized Intensity
0.0
0.5
1.0
1.5
2.0
2.5
3.0
Time (ms)

Figure 8:

Conflict of interest

The authors declare there are no conflict of interest

***Declaration of Interest Statement**

Declaration of interests

☒ The authors declare that they have no known competing financial interests or personal relationships that could have appeared to influence the work reported in this paper.

☐The authors declare the following financial interests/personal relationships which may be considered as potential competing interests: